Proceedings of the 11th Brazilian Congress of Thermal Sciences and Engineering – ENCIT 2006
Braz. Soc. of Mechanical Sciences and Engineering – ABCM, Curitiba, Brazil, Dec. 5-8, 2006

Paper CIT06-0856

NUMERICAL STUDY OF DISLOCATION MICROSTRUCTURES IN MATERIALS SUBJECTED TO CYCLIC LOADING USING THE WALGRAEF-AIFANTIS MODEL

Daniel Walgraef
Center for Nonlinear Phenomena and Complex Systems, CP-231,
Université Libre de Bruxelles, B-1050, Brussels, Belgium
dwaelgr@ulb.ac.be, dwalgraef@hotmail.com

José Pontes
Metallurgy and Materials Engineering Department, EP/COPPE
Federal University of Rio de Janeiro, P.O. Box 68505, 21941-972, Rio de Janeiro, RJ, Brazil
jopontes@metalmat.ufrj.br

Abstract. *Strain localization and dislocation pattern formation are typical features of plastic deformation in metals and alloys. Glide and climb dislocation motion along with accopanying production/annihilation processes of dislocations lead to the occurence of of instabilities of initially uniform dislocation distributions. These instabilities result into the development of various types of dislocation microstructures, such as dislocation cells, slip and kink bands, persistent slip bands, labyrinth structures, etc., depending on the externally applied loading and the intrinsic lattice constraints. The Walgraef-Aifantis (WA) model is an exemple of a reaction-diffusion model of coupled nonlinear equations which describe microstructure formation of forest (immobile) and gliding (mobile) dislocation densities in the presence of cyclic loading. This paper briefly discusses two versions of the WA model and focus on a finite differences, second order in time Cranck-Nicholson semi-implicit scheme, with internal iterations at each time step, for solving the model evolution equations in two dimensions..*

keywords: *dislocation patterns, nonlinear dynamics, fatigue*

1. The Walgraef-Aifantis (WA) model

In the spirit of earlier dislocation models derived for exemple by Ghoniem *et al.* (1990) for creep, or by Walgraef and Aifantis (1985, 1986, 1997), by Schiller and Walgraef (1988), and by Kratochvil (1979), for dislocation microstructure formation in fatigue, the dislocation population is divided into static dislocations, which may result from work hardening and consist in the nearly immobile dislocations of the "forest", of subgrains walls or boundaries, etc., and the mobile dislocations which glide between these obstacles. One has thus to derive coupled rate equations for the static and mobile dislocation densities, ρ_s and ρ_m. For the sake of simplicity, we shall consider single crystals, oriented for single slip. These dislocations are related to the plastic strain rate via the Orowan relation:

$$\dot{\epsilon}_p = b\rho_m v_g \tag{1}$$

where b is the length of the Burgers vector, ρ_m is the total mobile dislocation density and v_g is the glide velocity in the primary slip band. Time is measured in cycles of loading. Although this relation is, in principle, valid for mean values we will consider that it is also valid locally.

The internal stress is defined by the relation:

$$\sigma_i = \frac{\mu b}{2\pi\lambda} + \xi\mu b\sqrt{\rho_s} \tag{2}$$

where the first contribution comes frm obstacles such as precipitates or pre-existing walls separated by an effective spacing λ (μ is the shear modulus). The second part is the contribution from the static dislocation population which also opposes dislocation motion. The internal strees reduces the effective stress acting on the dislocations and is defined as:

$$\sigma_e = \sigma_a - \sigma_i \tag{3}$$

where σ_a is the applied stress. Finally, the glide velocity is related to the effective stress via appropriate phenomenological relations expressing the fact that individual dislocation motion is initiated when the effective stress acting on a dislocation exceeds the yeld stress. One may consider, for exemple:

$$v_g \propto \sigma_e - \sigma_0 \quad (\sigma_e > \sigma_0) \tag{4}$$

$$v_g = 0 \quad (\sigma_e < \sigma_0) \tag{5}$$

where σ_0 is the yeld strength.

The essential features of the dislocation dynamics in the plastic regime are, on the one side, their mobility, dominated by plastic flow, but which also includes theremal diffusion and climb, and, on the other side, their mutual interaction process, the more important being:

- Multiplication of static dislocations within the forest;
- Static recovery in the forest via static-static anihilation processes;
- Freeing of static dislocations: when the effective stress increases and exceeds some threshold, it disturbs the local structure of the forest and, in particular, destabilize dislocation clusters which decompose into mobile dsilocations. The freeing of forest dislocations occurs with a rate β, which depends on the aplied stresses and material parameters;
- Pinning of mobile dislocation by the forest. Effectively, mobile dislocations may be immobilized by the various dislocation clusters forming the forest. The dynamical contribution of such processes is of the form $G(\rho_s)\rho_m$, where $G(\rho_s) = g_n\rho_s^n$ is the pinning rate of a mobile dislocation by a cluster of n static ones. The Walgraef-Aifantis (WA) model considers $n = 2$.

The resulting dynamical system may then be written as:

$$\frac{\partial \rho_s}{\partial t} = D_s\nabla^2\rho_s + \sigma - v_s d_c \rho_s^2 - \beta\rho_s + \gamma\rho_s^2\rho_m \tag{6}$$

$$\frac{\partial \rho_m}{\partial t} = D_m\nabla_x^2\rho_m + \beta\rho_s - \gamma\rho_s^2\rho_m \tag{7}$$

where D_s represents the effective diffusion within the forest resulting from the thermal mobility and climb and D_m represents the effective diffusion resulting from the glide of mobile dislocations between obstacles ($D_m \gg D_s$). The diffusion coefficient D_m is positive in the present case, but it may become negative, when sweeping or correlation effects are taken into account (Kratochvil and Saxlova), leading to the instability of uniform forest dislocations from the very beginning. The coefficient d_c is the characteristic length of spontaneous dipole collapse. This length, or at least its order of magnitude, may be, in principle, evaluated from microscopic analysis (Mughrabi, 1979). β is the rate of dislocation freeing from the forest and is associated with the destabilization of dislocation dipoles or clusters under stress. Numerical dislocation dynamics simulations show that in BBC crystals, for exemple, there is a critical value of external applied stresses above which dislocation dipoles become unstable. This value is a decreasing function of the distance between dipole slip lines. If the forest may be considered as an ensemble of dipoles with a mean characteristic width, the treshold stress for destabilization, or freeing, σ_f, could be extracted from such simulatins. More extended numerical analysis could include higher order dislocation clusters and provide the dependence of the threshold strss on the forest dislocation densitty. The freeing rate is should thus be zero below the freeing threshold, and an increasing functionof the applied stress above it. Hence, $\beta \approx \beta_0(\sigma_a - \sigma_f)^n$ for $\sigma_a > \sigma_f$, n being a phenomenological parameter.

2. The modified WA model: effect of gradient terms

The approximation of mobile dislocation diffusion is controversial and may be lifted. To do so, the mobile dislocation density, ρ_m is divided into two subfamilies representing the dislocation gliding in the direction of the Burgers vector (ρ_m^+) and in the opposite one (ρ_m^-), with $\rho_m = \rho_m^+ + \rho_m^-$.

For crystals with well-developed forest density, and oriented for single slip, we now write (with v_g oriented along the x direction):

$$\frac{\partial \rho_s}{\partial t} = D_s\nabla^2\rho_s + \sigma - v_s d_c \rho_s^2 - \beta\rho_s + \gamma\rho_s^2\rho_m \tag{8}$$

$$\frac{\partial \rho_m^+}{\partial t} = -\nabla_x v_g \rho_m^+ + \frac{\beta}{2}\rho_s - \gamma\rho_s^2\rho_m^+ \tag{9}$$

$$\frac{\partial \rho_m^-}{\partial t} = \nabla_x v_g \rho_m^- + \frac{\beta}{2}\rho_s - \gamma\rho_s^2\rho_m^- \tag{10}$$

or:

$$\frac{\partial \rho_s}{\partial t} = D_s \nabla^2 \rho_s + \sigma - v_s d_c \rho_s^2 - \beta \rho_s + \gamma \rho_s^2 \rho_m \tag{11}$$

$$\frac{\partial \rho_m}{\partial t} = -\nabla_x v_g \rho_m + \frac{\beta}{2} \rho_s - \gamma \rho_s^2 \rho_m \tag{12}$$

$$\frac{\partial \sigma_m^-}{\partial t} = -\nabla_x v_g \rho_m - \gamma \rho_s^2 \sigma_m \tag{13}$$

where $\sigma_m = \rho_m^+ - \rho_m^-$ is the density of geometrically necessary dislocations. This variables evolves faster than the other two and may be adiabatically eliminated, leading to the following system, which includes a nonlinear diffusion term in the equation of ρ_m:

$$\frac{\partial \rho_s}{\partial t} = D_s \nabla^2 \rho_s + \sigma - v_s d_c \rho_s^2 - \beta \rho_s + \gamma \rho_s^2 \rho_m \tag{14}$$

$$\frac{\partial \rho_m}{\partial t} = \nabla_x \frac{v_g}{\gamma \rho_s^2} \nabla_x v_g \rho_m + \beta \rho_s - \gamma \rho_s^2 \rho_m \tag{15}$$

3. The numerical scheme for solving the WA model

In order to solve the modified WA model, we use a numerical scheme based on a one proposed by Christov and Pontes (2002). Equations (14) and (15) are solved numerically in two-dimensional rectangular domains, through the finite difference method, using a grid of uniformly spaced points, a second order in time Cranck-Nicholson semi-implicit method with internal interations at each time step, due to the nonlinear nature of the implicit terms. The proposed scheme is splitted in two equations using the Stabilizing Correction scheme (Christov and Pontes, 2002, Yanenko, 1971). The first half-step comprises implicit derivatives with respect to x and explicit derivatives with respect to y. In the second half-step, the derivatives with respect to y are kept implcit and those with respect to x are explicit. The splitting scheme is shown to be equivalent to the original one.

3.1. The target scheme

The target second order in time, Cranck-Nicholson semi-implicit scheme is:

$$\frac{\rho_s^{n+1} - \rho_s^n}{\Delta t} = \Lambda_x^{n+1/2} \frac{\rho_s^{n+1} + \rho_s^n}{2} + \Lambda_y^{n+1/2} \frac{\rho_s^{n+1} + \rho_s^n}{2} + f_1^{n+1/2} \tag{16}$$

$$\frac{\rho_m^{n+1} - \rho_m^n}{\Delta t} = \Lambda_2^{n+1/2} \frac{\rho_m^{n+1} + \rho_m^n}{2} + f_2^{n+1/2} \tag{17}$$

where n is the number of the time step. Upon including the $1/2$ factor in the operators $\Lambda_x^{n+1/2}$, $\Lambda_y^{n+1/2}$ and $\Lambda_2^{n+1/2}$, we obtain:

$$\frac{\rho_s^{n+1} - \rho_s^n}{\Delta t} = \Lambda_x^{n+1/2} \left(\rho_s^{n+1} + \rho_s^n\right) + \Lambda_y^{n+1/2} \left(\rho_s^{n+1} + \rho_s^n\right) + f_1^{n+1/2} \tag{18}$$

$$\frac{\rho_m^{n+1} - \rho_m^n}{\Delta t} = \Lambda_2^{n+1/2} \left(\rho_m^{n+1} + \rho_m^n\right) + f_2^{n+1/2} \tag{19}$$

The operators $\Lambda_x^{n+1/2}$, $\Lambda_y^{n+1/2}$ and $\Lambda_2^{n+1/2}$ and the functions $f_1^{n+1/2}$ and $f_2^{n+1/2}$ are defined as:

$$\Lambda_x^{n+1/2} = \frac{D_s}{2} \frac{\partial^2}{\partial x^2} - \frac{1}{4} v_s d_c \left(\frac{\rho_s^{n+1} + \rho_s^n}{2} \right) - \frac{\beta}{4} \tag{20}$$

$$\Lambda_y^{n+1/2} = \frac{D_s}{2} \frac{\partial^2}{\partial x^2} - \frac{1}{4} v_s d_c \left(\frac{\rho_s^{n+1} + \rho_s^n}{2} \right) - \frac{\beta}{4} \tag{21}$$

$$f_1^{n+1/2} = \sigma + \frac{\gamma}{2} \left(\frac{\rho_s^{n+1} + \rho_s^n}{2} \right)^2 \left(\rho_m^{n+1} + \rho_m^n\right) \tag{22}$$

$$\Lambda_2^{n+1/2} = \frac{1}{2} \frac{\partial}{\partial x} \left[\frac{v_g}{\gamma \left[\left(\rho_s^{n+1} + \rho_s^n\right)/2 \right]^2} \frac{\partial}{\partial x} v_g \right] - \gamma \left(\frac{\rho_s^{n+1} + \rho_s^n}{2} \right)^2 \tag{23}$$

$$f_2^{n+1/2} = \beta \left(\frac{\rho_s^{n+1} + \rho_s^n}{2} \right) \tag{24}$$

3.2. Internal iterations

Since the operators $\Lambda_x^{n+1/2}$, $\Lambda_x^{n+1/2}$ and $\Lambda_2^{n+1/2}$, as well as the functions $f_1^{n+1/2}$ and $f_2^{n+1/2}$ contain terms in the new stage, we do internal iterations at each time step, according to:

$$\frac{\rho_s^{n,k+1}-\rho_s^n}{\Delta t} = \Lambda_x^{n+1/2}\left(\rho_s^{n,k+1}-\rho_s^n\right)+\Lambda_y^{n+1/2}\left(\rho_s^{n,k+1}-\rho_s^n\right)+f_1^{n+1/2} \tag{25}$$

$$\frac{\rho_m^{n,k+1}-\rho_m^n}{\Delta t} = \Lambda_2^{n+1/2}\left(\rho_m^{n,k+1}\rho_m^n\right)+f_2^{n+1/2} \tag{26}$$

where the superscript $(n,k+1)$ identifies the "new" iteration, (n,k) and n stand for the values obtained in the previous iteration and in the previous time step, respectively. The operators $\Lambda_x^{n+1/2}$, $\Lambda_y^{n+1/2}$, $\Lambda_2^{n+1/2}$ and the functions $f_1^{n+1/2}$ and $f_2^{n+1/2}$ are redefined as:

$$\Lambda_x^{n+1/2} = \frac{D_s}{2}\frac{\partial^2}{\partial x^2}-\frac{1}{4}v_s d_c S^{n+1/2}-\frac{\beta}{4} \tag{27}$$

$$\Lambda_y^{n+1/2} = \frac{D_s}{2}\frac{\partial^2}{\partial x^2}-\frac{1}{4}v_s d_c S^{n+1/2}-\frac{\beta}{4} \tag{28}$$

$$f_1^{n+1/2} = \sigma+\frac{\gamma}{2}\left(S^{n+1/2}\right)^2\left(\rho_m^{n,k}+\rho_m^n\right) \tag{29}$$

$$\Lambda_2^{n+1/2} = \frac{\partial}{\partial x}\left(\frac{v_g}{2\gamma\left(S^{n+1/2}\right)^2}\frac{\partial}{\partial x}v_g\right)-\gamma\left(S^{n+1/2}\right)^2 \tag{30}$$

$$f_2^{n+1/2} = \beta S^{n+1/2}, \qquad \text{where: } S^{n+1/2}=\frac{\rho_s^{n,k}+\rho_s^n}{2} \tag{31}$$

The iterations proceed until the following criteria is satisfied:

$$\frac{\max||\rho_s^{n,K+1}-\rho_s^{n,K}||}{\max||\rho_s^{n,K}||}<\delta \qquad \text{and} \qquad \frac{\max||\rho_m^{n,K+1}-\rho_m^{n,K}||}{\max||\rho_m^{n,K}||}<\delta$$

in all grid points, for a certain K. Then the last iteration gives the value of the sought functions in the "new" time step, $\rho_s^{n+1}\stackrel{\text{def}}{=}\rho_s^{n,K+1}$ et $\rho_m^{n+1}\stackrel{\text{def}}{=}\rho_s^{n,K+1}$.

3.3. The splitting of the ρ_s equation

The splitting of Eq. (25) is made according to:

$$\frac{\tilde{\rho}_s-\rho_s^n}{\Delta t} = \Lambda_x^{n+1/2}\,\tilde{\rho}_s+\Lambda_y^{n+1/2}\,\rho_s^n+f_1^{n+1/2}+\left(\Lambda_x^{n+1/2}+\Lambda_y^{n+1/2}\right)\rho_s^n \tag{32}$$

$$\frac{\rho_s^{n,k+1}-\tilde{\rho}_s}{\Delta t} = \Lambda_y^{n+1/2}\left(\rho_s^{n,k+1}-\rho_s^n\right) \tag{33}$$

In order to show that the splitting represents the original scheme, we rewrite Eqs. (32) and (33) in the form:

$$\left(E-\Delta t\,\Lambda_x^{n+1/2}\right)\tilde{\rho}_s=\left(E+\Delta t\,\Lambda_y^{n+1/2}\right)\rho_s^n+\Delta t\,f_1^{n+1/2}+\left(\Delta t\,\Lambda_x^{n+1/2}+\Delta t\,\Lambda_y^{n+1/2}\right)\rho_s^n \tag{34}$$

$$\left(E-\Delta t\,\Lambda_y^{n+1/2}\right)\rho_s^{n,k+1}=\tilde{\rho}_s-\Delta t\,\Lambda_y^{n+1/2}\rho_s^n \tag{35}$$

where E is the unity operator. The intermediate variable $\tilde{\rho}_s$ is eliminated by applying the operator $\left(E-\Delta t\,\Lambda_x^{n+1/2}\right)$ to the second equation and by summing the result to the first one:

$$\left(E-\Delta t\,\Lambda_x^{n+1/2}\right)\left(E-\Delta t\,\Lambda_y^{n+1/2}\right)\rho_s^{n,k+1}=\left(E+\Delta t\,\Lambda_y^{n+1/2}\right)\rho_s^n- \tag{36}$$

$$\left(E-\Delta t\,\Lambda_x^{n+1/2}\right)\Delta t\,\Lambda_y^{n+1/2}\rho_s^n+\Delta t\,f_1^{n+1/2}+\left(\Delta t\,\Lambda_x^{n+1/2}+\Delta t\,\Lambda_y^{n+1/2}\right)\rho_s^n \tag{37}$$

this result may be rewritten as:

$$\left(E+\Delta t^2\,\Lambda_x^{n+1/2}\Lambda_y^{n+1/2}\right)=\Delta t\left(\Lambda_x^{n+1/2}+\Lambda_y^{n+1/2}\right)\left(\rho_s^{n,k+1}+\rho_s^n\right)+\Delta t\,f_1^{n+1/2}$$

or either:

$$\left(E+\Delta t^2\,\Lambda_x^{n+1/2}\Lambda_y^{n+1/2}\right)\frac{\rho_s^{n,k+1}-\rho_s^n}{\Delta t}=\left(\Lambda_x^{n+1/2}+\Lambda_y^{n+1/2}\right)\frac{\rho_s^{n,k+1}-\rho_s^n}{2}+f_1^{n+1/2} \tag{38}$$

A comparison with Eq. (25) shows that Eq. (38) is actually equivalent to the first one except by the defined positive operator having a norm greater than one,

$$B \equiv E + \Delta t^2 \, \Lambda_x^{n+1/2} \Lambda_y^{n+1/2} = E + \mathcal{O}\left(\Delta t^2\right)$$

which acts on the term $\left(\rho_s^{n,k+1} - \rho_s^n\right)/\Delta t$. This means that this operator does not change the steady state solution. Furthermore, since $||B|| > 1$ the spliting scheme is more stable than the original scheme.

3.4. Spatial discretization

The grid is "staggered" and the discretization of the diffusive term of Eq. (15) is made according to the following formula, which preserves the conservation law implicit in the divergence:

$$\Delta t \frac{\partial}{\partial x}\left[\frac{v_g}{\gamma \rho_s^2}\frac{\partial}{\partial x} v_g \rho_m\right] \approx \Delta t \frac{\partial}{\partial x}\left[\frac{v_g}{\gamma (S^{n+1/2})^2}\frac{\partial}{\partial x} v_g \frac{\rho_m^{n,k+1} + \rho_m^n}{2}\right]$$

Upon writting:

$$Q_{i,j} = \frac{\Delta t \, v_g}{4\gamma (S_{i,j}^{n+1/2})^2}$$

we replace the diffusive term of ρ_m by:

$$\frac{\Delta t}{2}\frac{\partial}{\partial x}\left[\frac{v_g}{\gamma \rho_s^2}\frac{\partial}{\partial x} v_g \rho_m\right] \approx \tag{39}$$

$$\left(Q_{i,j} + Q_{i,j+1}\right)\frac{v_g}{\Delta x}\left((\rho_m)_{i,j+1} - (\rho_m)_{i,j}\right) - \left(Q_{i,j-1} + Q_{i,j}\right)\frac{v_g}{\Delta x}\left((\rho_m)_{i,j} - (\rho_m)_{i,j-1}\right) = \tag{40}$$

$$\left(Q_{i,j-1} + Q_{i,j}\right)\frac{v_g}{\Delta x}(\rho_m)_{i,j-1} - \left(Q_{i,j-1} - 2Q_{i,j} + Q_{i,j+1}\right)(\rho_m)_{i,j} + \left(Q_{i,j} + Q_{i,j+1}\right)(\rho_m)_{i,j+1} \tag{41}$$

The diffusive terms of Eq. (14) are written in discrete form by using the usual three points centred formula, of second order. Neumann boundary conditions are used in the integration of the WA model, with derivatives in the direction perpendicular to the walls equal to zero. The algebraic linear systems were solved using a routine with gaussian elimination and pivoting, written by C. I. Christov, from the University of Louisiana at Lafayette.

4. Results

We present the result of one simulation with the nonlinear difusion of ρ_m, run in a square box with $20\mu m \times 5\mu m$, using a grid containning 3000×750 points. The initial condition consists of the time independent uniform base state plus a random with zero mean.

The model parameters adopted in the simulation are $v_s = 1\mu m \, cm^{-1}$, $d_c = 2.5^{-2}\mu m$, $D_s = 3\times 10^{-3}\mu m^2 cy^{-1}$, $v_g = 10^2 \mu m \, cy^{-1}$, $\gamma = 2 \times 10^{-2}$, $\sigma = 250 \mu m^{-2} cy^{-1}$. The simulations were run with a time step of $2.5 \times 10^{-3} cy$.

During the simulations, we monitore the velocity of evolution of the patterns, by measuring:

$$L_1 = \frac{1}{\Delta t}\frac{\sum_{ij}|\rho_s^{n+1} - \rho_s^n| + \sum_{ij}|\rho_m^{n+1} - \rho_m^n|}{\sum_{ij}|\rho_s^{n+1}| + \sum_{ij}|\rho_m^{n+1}|} \tag{42}$$

where the summations are made over all points (i, j) of the grid. The simulations proceeded while the velocity of evolution of the patterns is above a specified value.

The results are presented in the followig figures. Figs. (1) to (4) show selected frames of the time evolution of ρ_s. The simulation evolves to a set of walls parallel to the slip direction. Fig. (6) shows the time evolution of L_1, the number of iterations per time step and the evolution of the maximum of ρ_s.

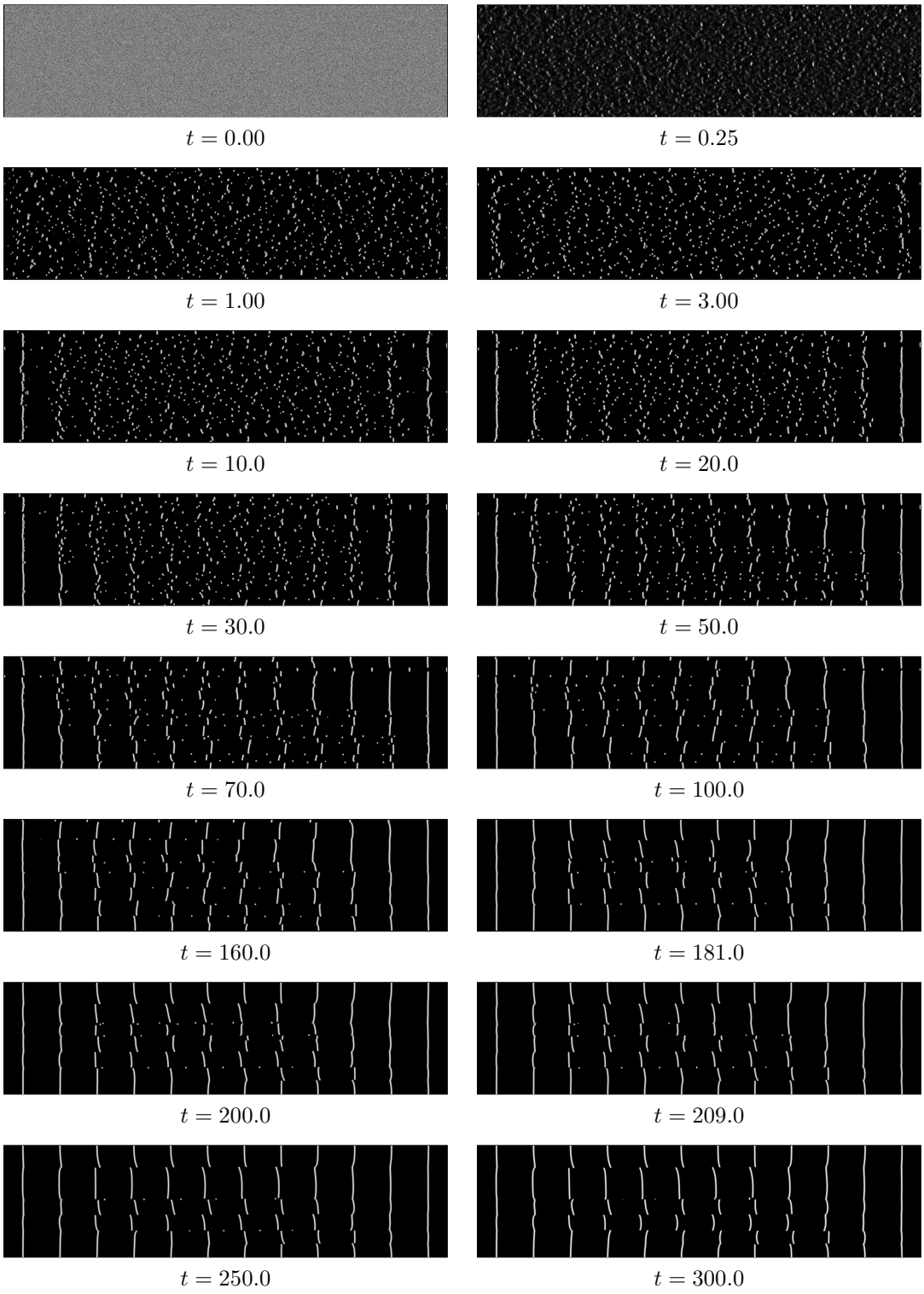

Figure 1: Time evolution of ρ_s (part 1).

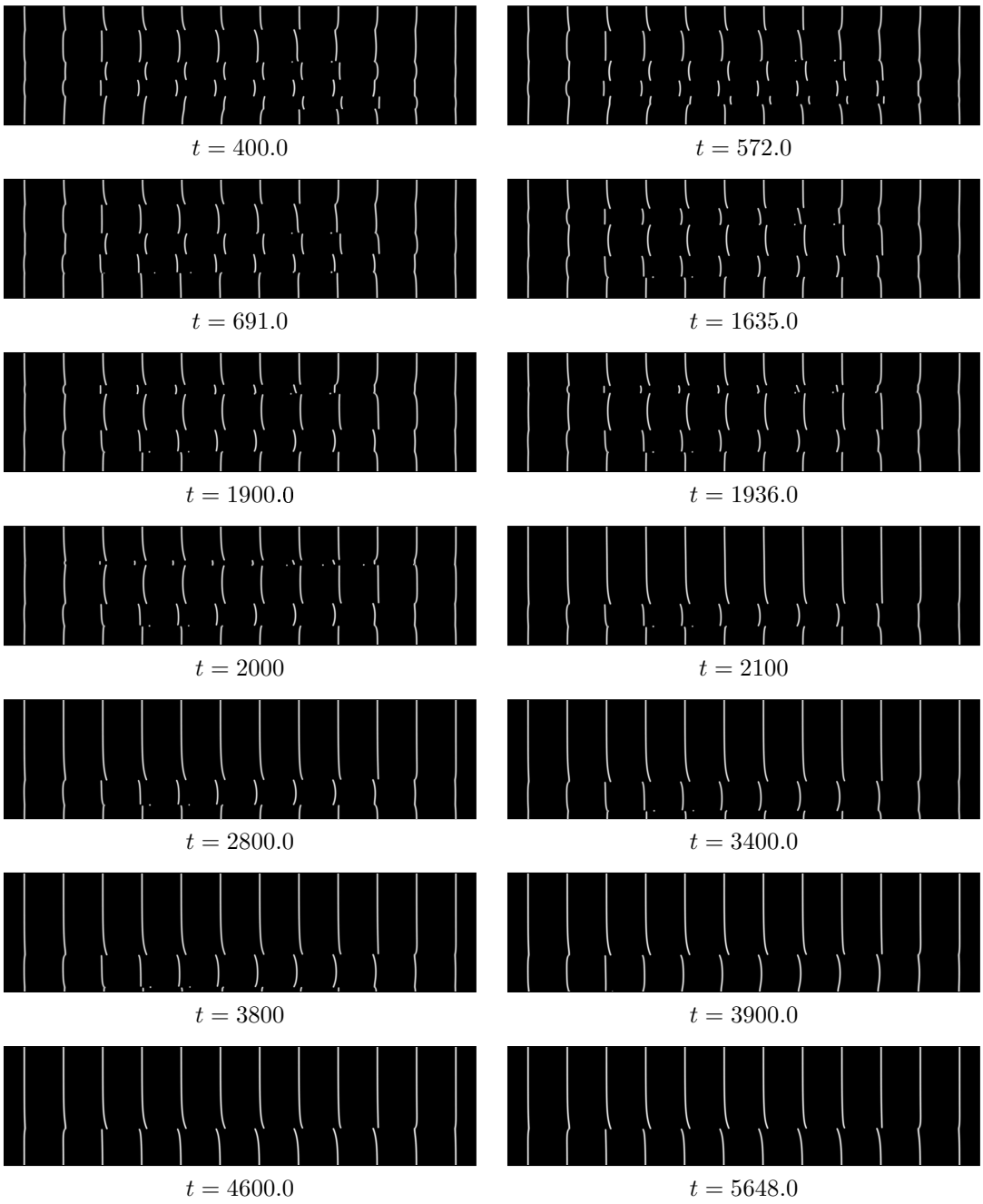

Figure 2: Time evolution of ρ_s (part 2).

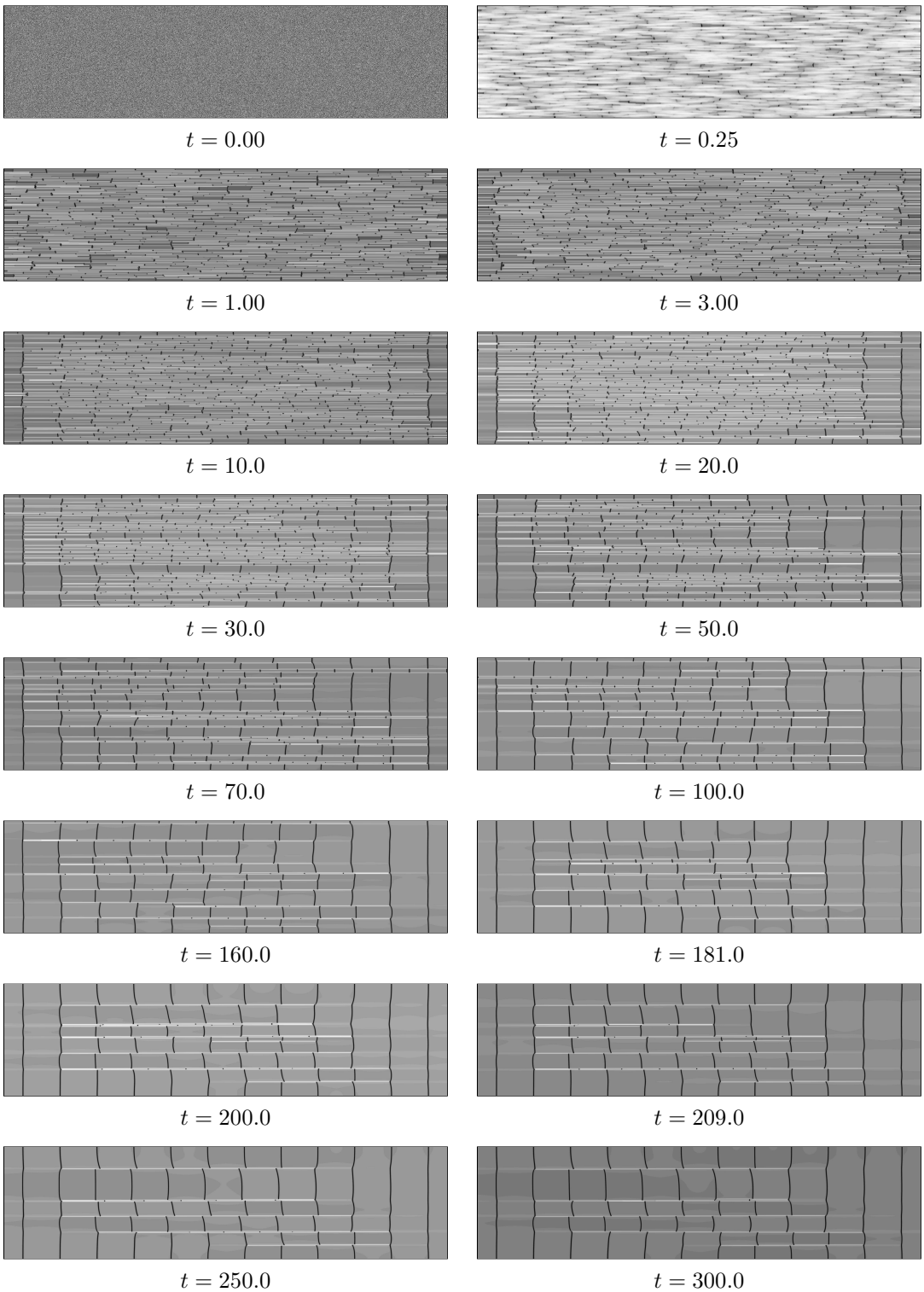

Figure 3: Time evolution of ρ_m (part 1).

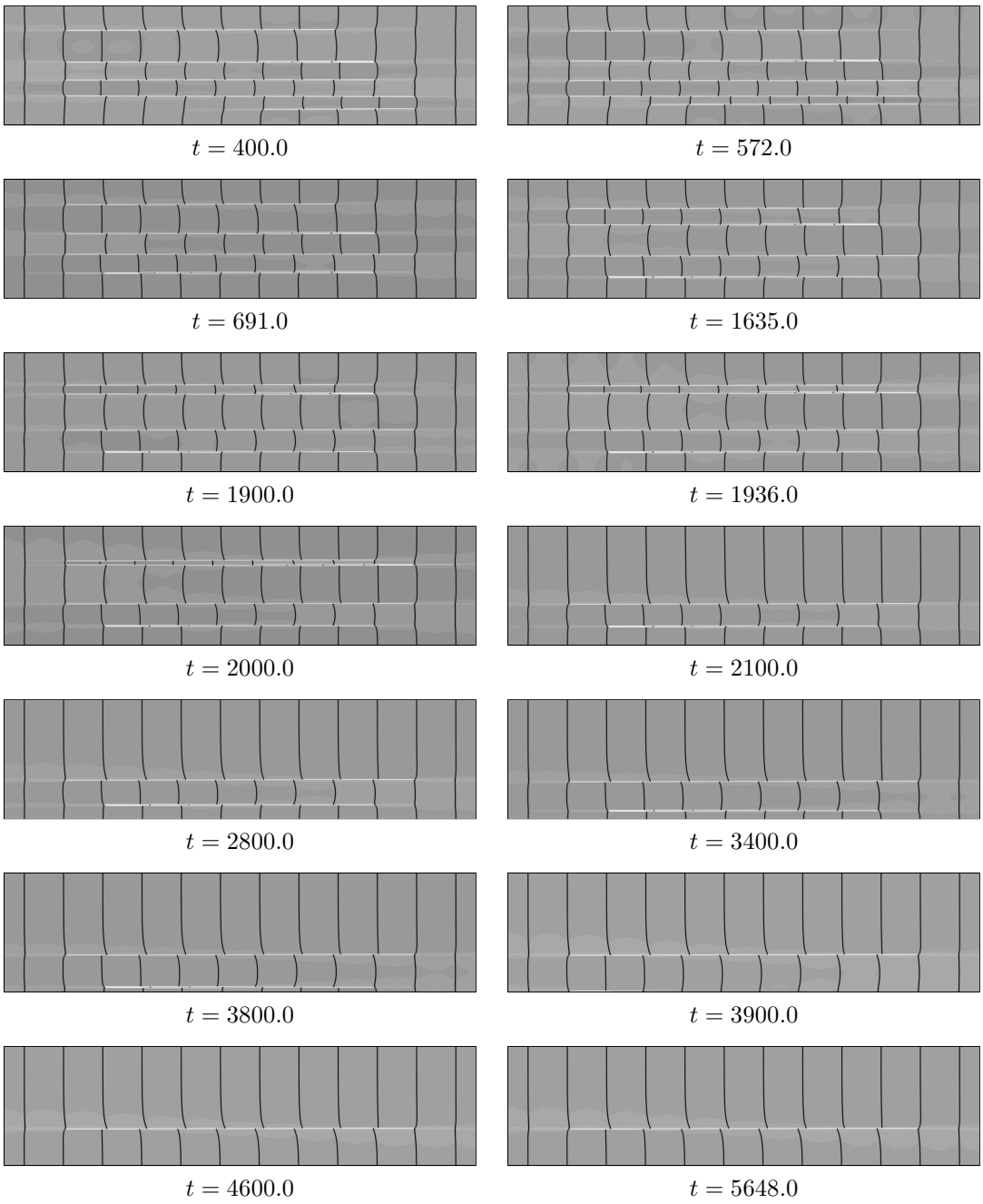

Figure 4: Time evolution of ρ_s (part 2).

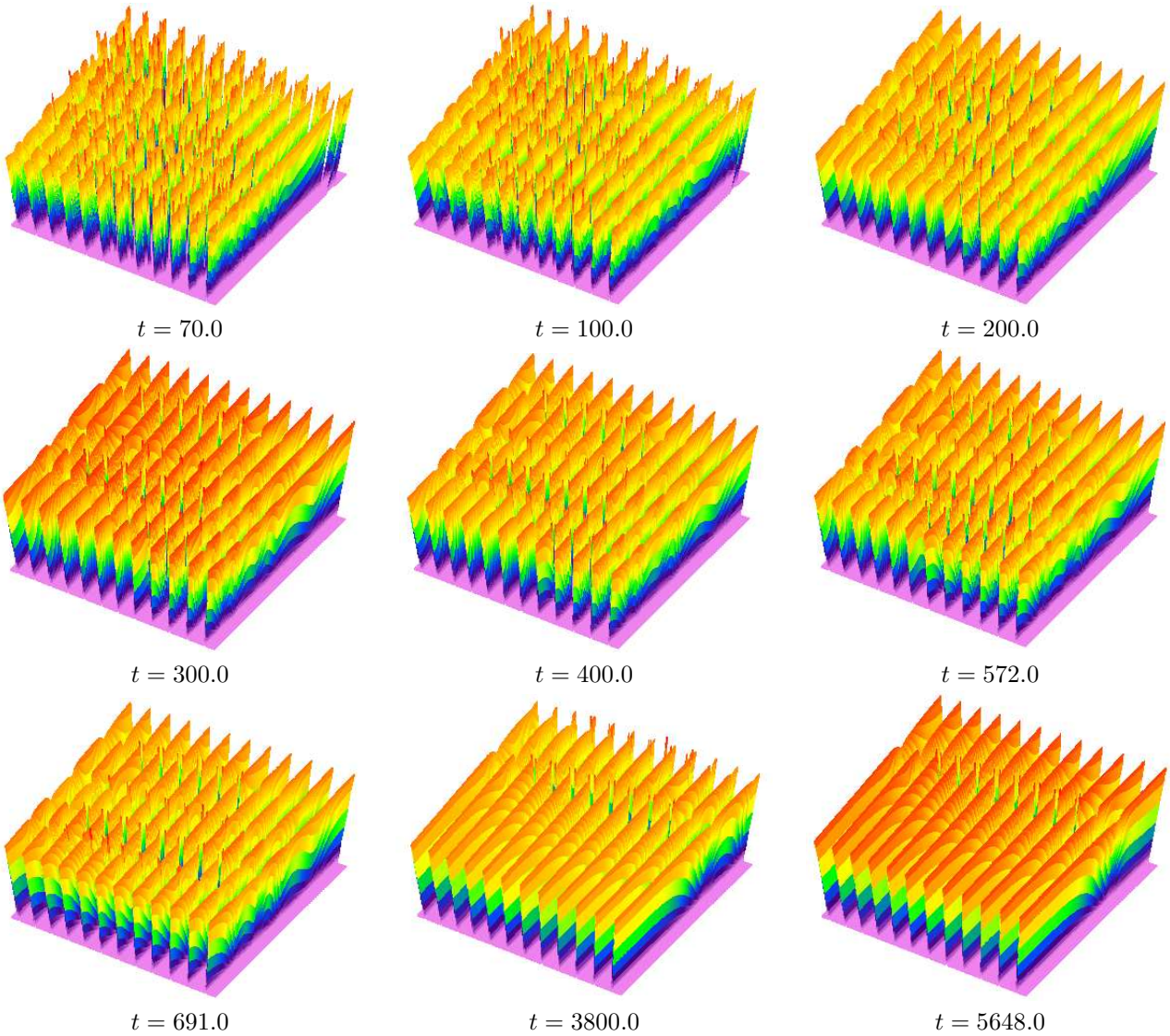

Figure 5: 3D figures of the time evolution of ρ_s.

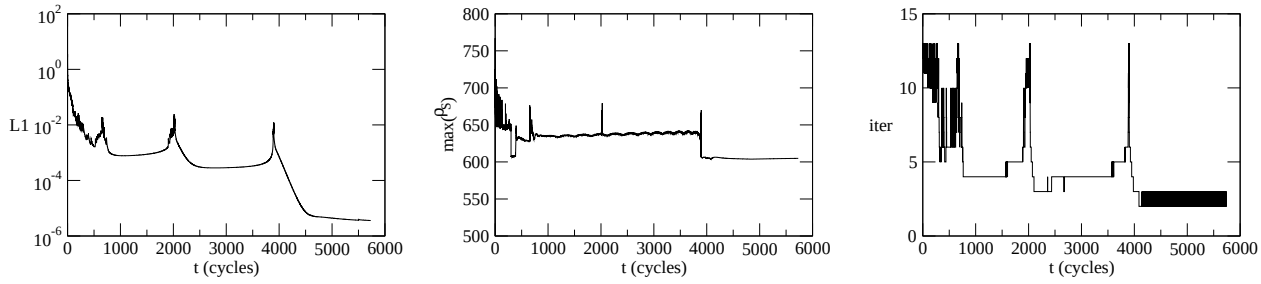

(a) (b) (c)

Figure 6: Curves of $L_1 \times t$, $max(\rho_s) \times t$ and number of iterations $\times t$.

5. Acknowledgements

The authors warmfully acknowledge the Center of Parallel Computing of the Federal University of Rio the Janeiro (NACAD/COPPE/UFRJ) and to prof. Alvaro L.G.A. Coutinho for the use of a cluster where the simulations presented where made. JP also acknowledges prof. C. I. Christov, from the University of Louisiana at Lafayette. The numerical scheme here proposed is based on his ideas.

6. References

Christov, C. I. and Pontes, J., 2002, Numerical Scheme for Swift-Hohenberg Equation with Strict Implementation of Lyapunov Functional, "Mathematical and Computer Modelling", Vol. 35, pp. 87–99.

Ghoniem, N. M., Matthews, J. R., and Amoedo, R. J., 1990, "Res Mechanica", Vol. 29, pp. 197.

Kratochvil, J., 1988, On stability of dislocation structures in cyclically deformed metal crystals and formation of persistent slip bands, "Rev. Phys. Apliquée", Vol. 23, pp. 419.

Mughrabi, H., Ackermann, F., and Herz, K., 1979, Fong, E. T., editor, "Fatigue Mechanisms, ASTM-NBS-NSF Symposium", Kansas City. ASTM, paper No. STP-675.

Pontes, J., Walgraef, D., and Aifantis, E. C., 2006, On dislocation patterning: multiple slip effects in the rate approach, "Int. J. Plasticity", Vol. 22, No. 8, pp. 1486–1505.

Schiller, C. and Walgraef, D., 1988, Numerical simulation of persistent slip band formation, "Acta Metall.", Vol. 36, No. 2, pp. 563–574.

Walgraef, D., 1997, "Spatio-Temporal Pattern Formation", Springer, New York.

Walgraef, D. and Aifantis, E. C., 1985, Dislocation Patterning as the Result of Dynamical Instabilities, "J. Appl. Phys.", Vol. 58, pp. 668.

Walgraef, D. and Aifantis, E. C., 1986, On the formation and stability of dislocation patterns, "Int. J. Eng. Sci.", Vol. 23, pp. 1351, 1359 and 1364.

Walgraef, D. and Pontes, J., 2005, Numerical simulation of dislocation dynamics in materials subjected to cyclic loading, with the Walgraef-Aifantis model, "Anais do VII Encontro Modelagem Computacional", Nova Friburgo, RJ, Brasil. Instituto Politécnico/UERJ, (in CD - ISBN).

Yanenko, N. N., 1971, "The Method of Fractional Steps", Springer, New York.